

## Stability of stripe magnetic domain in magnetic multilayers: Prediction and observation

Sug-Bong Choe and Sung-Chul Shin

*Department of Physics and Center for Nanospinics of Spintronic Materials, Korea Advanced Institute of Science and Technology, Taejon 305-701, Korea*

(Received 22 July 1998)

We present an analytical theory of the magnetic domain configuration in magnetic multilayers. The theory predicts a sharp transition from a large-areal domain pattern to a striped domain configuration as a function of increasing magnetic layer thickness. This transition was verified experimentally by direct magnetic domain observations in Co/Pd multilayers. This transition results from a competition between the magnetostatic energy and the exchange and anisotropy energies.

[S0163-1829(99)15001-X]

Magnetic multilayers are artificially grown periodic structures of alternating layers of magnetic and nonmagnetic constituents.<sup>1</sup> Interest in these systems has grown rapidly in recent years motivated in part by the search for new magnetic materials of technological interest,<sup>2,3</sup> and in part by their novel magnetic properties. In spite of numerous studies of these systems very few have addressed their magnetic domain structures.<sup>4,5</sup> However, a proper understanding of their magnetic domain configurations will provide fundamental insights as well as help to achieve the technical objectives of these systems, since magnetization reversal mechanism is closely related with their magnetic domain structures.

The magnetostatic energy of the magnetic domain structures in magnetic multilayered systems has yet to be investigated due to the complexity of this long-range magnetic interaction. The magnetostatic energy is one of the major constituents in determining the domain configuration in multilayers because the magnetostatic energy in ultrathin multilayers is much enhanced by high density of magnetic poles at interfaces. The magnetostatic energy of ultrathin magnetic layers having one or several atomic layers has been considered by Yafet and Gyorgy<sup>6</sup> based on dipole interaction between magnetic atoms. Kamberský *et al.*<sup>7</sup> have simulated the domain structure in multilayers by an iterative relaxation method. Recently, we have developed an explicit method to calculate the magnetostatic energy in multilayered structures with perpendicular magnetic anisotropy by solving Maxwell's equations in continuum approximation. In this paper, we take advantage of this method to include the contribution from the magnetostatic energy in calculating the magnetic domain configurations in magnetic multilayers within an analytical theory. In this theory, the finite size of the domain-wall transition is explicitly included. The present theory has been applied to Co/Pd multilayered system and found to quantitatively explain the transition of the magnetic domain configuration.

We modeled the multilayered structure stacked alternately along the  $z$  direction with magnetic sublayer  $A$  and nonmagnetic sublayer  $B$  lying in the  $XY$  plane as depicted in Fig. 1. The multilayered structure will be denoted by  $(t_A/t_B)_n$ , where  $t_A$  and  $t_B$  are the thicknesses of sublayers  $A$  and  $B$ , respectively, and  $n$  represents number of repeats. In the present model the magnetic properties of the multilayer are

characterized by the saturation magnetization  $M_A$ , the exchange stiffness  $A_A$ , and the magnetocrystalline anisotropy  $K_A$  of the magnetic sublayer  $A$ , as well as the surface anisotropy  $K_S$  caused by broken symmetry at the interface and the induced magnetization  $M_B$  of the sublayer  $B$ . Linear stripe domain was assumed to be infinitely long along the  $y$  axis and periodic along the  $x$  axis, but the interlayer variation along the  $z$  axis was ignored. A Bloch-type wall of the wall-transition width  $l$ , rather than a Néel-type wall, was considered because of its lower magnetostatic energy. For a given stripe-domain period  $d$ , the domain pattern  $\hat{\mathbf{m}}(x)$  can be transformed into Fourier series as

$$\begin{aligned} \hat{\mathbf{m}}(x) &= \cos[\theta(x)]\hat{\mathbf{z}} + \sin[\theta(x)]\hat{\mathbf{y}} \\ &= \sum_{k=-\infty}^{\infty} (C_k\hat{\mathbf{z}} + S_k\hat{\mathbf{y}})e^{i(2\pi kx/d)}, \end{aligned} \quad (1)$$

where  $\theta$  is the angle of the magnetization direction from the film normal and the Fourier coefficients  $C_k$  and  $S_k$  are obtained by numerical integration.

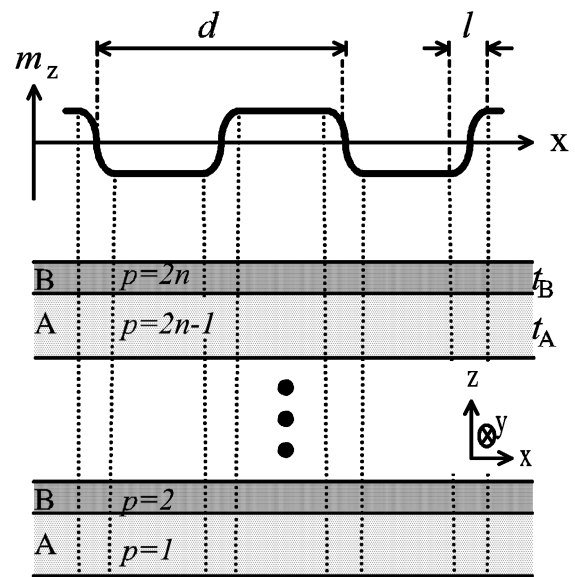


FIG. 1. Schematic diagram of the present model for the magnetic domain configuration in the multilayered structure.

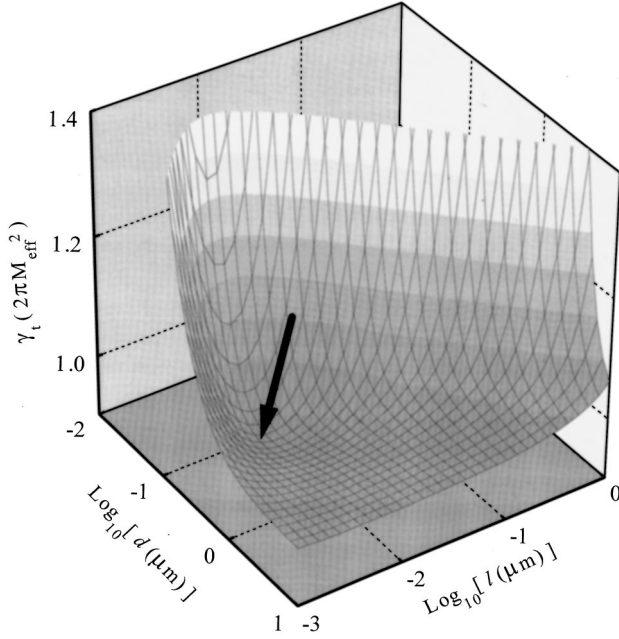


FIG. 2. The three-dimensional plot of  $\gamma_t$  as a function of  $d$  and  $l$  for  $(6\text{-\AA Co}/11\text{-\AA Pd})_{10}$  multilayer, where  $\gamma_t$  is normalized by the effective magnetostatic energy density  $2\pi M_{\text{eff}}^2$  of the saturated state. The minimum of  $\gamma_t$  is indicated by the arrow.

Considering uniaxial anisotropy composed of the magnetocrystalline anisotropy  $K_A$  and the surface anisotropy  $K_S$ , the anisotropy energy density  $\gamma_a$  of the multilayer is given by  $\gamma_a = -[(2K_S + t_A K_A)/d(t_A + t_B)] \int_{-d/2}^{d/2} \cos^2[\theta(x)] dx$ . After substituting  $\cos[\theta(x)]$  by Eq. (1) and then, using orthogonality of the trigonometric functions, the anisotropy energy density becomes

$$\gamma_a = -\frac{2K_S + t_A K_A}{t_A + t_B} \sum_{k=0}^{\infty} C_k^2. \quad (2)$$

The exchange energy density  $\gamma_x$  of the multilayer is given by  $\gamma_x = -[t_A A_A / 2a_A d(t_A + t_B)] \sum_{k=-d/2a_A}^{d/2a_A-1} \cos[\Delta\theta(ka_A)]$ , where  $a_A$  is the lattice constant of  $A$  atoms lying in the fcc lattice and  $\Delta\theta$  is the angle between the magnetization directions of two neighboring atoms. With continuum approximation of  $\Delta\theta(x) = \theta(x + a_A/2) - \theta(x - a_A/2)$  and substitution by Eq. (1), it can be rewritten as

$$\gamma_x = -\frac{t_A}{t_A + t_B} \frac{A_A}{2a_A^2} \sum_{k=0}^{\infty} (C_k^2 - S_k^2) \cos\left[\frac{2\pi k a_A}{d}\right]. \quad (3)$$

For the  $p$ th sublayer having the saturation magnetization  $M_p$  and the layer thickness  $t_p$  as shown in Fig. 1, the magnetic scalar potential  $\phi_p$  is given by

$$\phi_p^\dagger(x, z) = 4M_p d \sum_{k=1}^{\infty} \frac{C_k}{k} \sinh\left[\frac{\pi k t_p}{d}\right] e^{-(2\pi k z/d)} \cos\left[\frac{2\pi k x}{d}\right] + 2\pi M_p C_0 t_p,$$

for the upper region of the  $p$ th sublayer and

$$\phi_p^0(x, z) = 4M_p d \sum_{k=1}^{\infty} \frac{C_k}{k} \sinh\left[\frac{2\pi k z}{d}\right] e^{-(\pi k t_p/d)} \cos\left[\frac{2\pi k x}{d}\right] + 4\pi M_p C_0 z,$$

for the inside region of the sublayer by solving Maxwell's equations with boundary conditions, where  $z$  is the distance from the center of the sublayer.<sup>5</sup> The potential of the lower region  $\phi_p^\dagger$  is obtained by antisymmetric condition of  $\phi^\dagger(z) = -\phi^\dagger(-z)$ . The magnetostatic energy density  $e_q$  of the  $q$ th sublayer is given by

$$e_q = -(1/2dt_q) \int_{-d/2}^{d/2} \int_{-t_q/2}^{t_q/2} \vec{M}_q \cdot \hat{z} (\partial\Phi_q / \partial z) dz dx,$$

where the total magnetic scalar potential  $\Phi_q$  exerting on the inside of the  $q$ th sublayer is obtained by summing up  $\phi_p$  over the multilayer. Then, the magnetostatic energy density  $e_q^A$  of the alternating  $q$ th (odd number)  $A$  sublayer is rewritten as

$$e_q^A = 2\pi M_A^2 C_0^2 - \frac{dM_A^2}{t_A} \sum_{k=1}^{\infty} \frac{C_k^2}{k} \left\{ 2\alpha^k f_\alpha(k) + f_\alpha^2(k) \epsilon^{2k} \frac{2 - \epsilon^{k(q-1)} - \epsilon^{k(2n-q-1)}}{1 - \epsilon^{2k}} + \kappa f_\alpha(k) f_\beta(k) \epsilon^k \frac{2 - \epsilon^{k(q-1)} - \epsilon^{k(2n-q+1)}}{1 - \epsilon^{2k}} \right\},$$

where  $\alpha = e^{-\pi t_A/d}$ ,  $\beta = e^{-\pi t_B/d}$ ,  $f_\alpha(k) = \alpha^k - \alpha^{-k}$ ,  $f_\beta(k) = \beta^k - \beta^{-k}$ ,  $\epsilon = \alpha\beta$ , and  $\kappa = M_B/M_A$ . The magnetostatic energy  $e_r^B$  of the alternating  $r$ th (even number)  $B$  sublayer is also calculated by the same way. The total magnetostatic energy is then obtained by summing  $e_q^A$  and  $e_r^B$  over the multilayer and thus, the magnetostatic energy density  $\gamma_d$  of the multilayer can be rewritten as follows:

$$\gamma_d = 2\pi M_{\text{eff}}^2 C_0^2 - \frac{2dM_A^2}{t_A + t_B} \sum_{k=1}^{\infty} \frac{C_k^2}{k} \left\{ \alpha^k f_\alpha(k) + \kappa^2 \beta^k f_\beta(k) + [f_\alpha^2(k) + \kappa^2 f_\beta^2(k)] \frac{\epsilon^{2k}}{1 - \epsilon^{2k}} \left[ 1 - \frac{1}{n} \frac{1 - \epsilon^{2nk}}{1 - \epsilon^{2k}} \right] + 2\kappa f_\alpha(k) f_\beta(k) \frac{\epsilon^k}{1 - \epsilon^{2k}} \left[ 1 - \frac{1 + \epsilon^{2k}}{2n} \frac{1 - \epsilon^{2nk}}{1 - \epsilon^{2k}} \right] \right\}, \quad (4)$$

where  $2\pi M_{\text{eff}}^2 = 2\pi(t_A M_A^2 + t_B M_B^2)/(t_A + t_B)$ .

Now, the total domain energy  $\gamma_t$ , defined as  $\gamma_t(d, l) = \gamma_a(d, l) + \gamma_x(d, l) + \gamma_d(d, l)$ , is expressed as a function of  $d$  and  $l$  with the magnetic properties of a given multilayered structure. The  $\gamma_t(d, l)$  is a smooth function with a single minimum and therefore, in any multilayered structure it is possible to predict the ground state of the domain configuration by searching for a minimum  $\gamma_t$ . At first, we evaluate the values of  $N \times N$  mesh points over a certain range of  $d$  and  $l$ . Then, we reduce the scanning range of  $d$  and  $l$  around the minima point of the  $N \times N$  mesh. We repeat the evaluation of the values of  $N \times N$  mesh and the reduction of the range until

TABLE I. The values of the magnetic parameters of Co/Pd multilayers used in the calculation.

Magnetic parameters	Values
Exchange stiffness of Co, $A_{\text{Co}}$	$2.31 \times 10^{-6}$ erg/cm <sup>a</sup>
Magnetocrystalline anisotropy of Co, $K_{\text{Co}}$	$4.1 \times 10^6$ erg/cc <sup>a</sup>
Saturation magnetization of Co, $M_{\text{Co}}$	$1.45 \times 10^3$ emu <sup>a</sup>
Surface anisotropy, $K_S$	$0.77$ erg/cm <sup>2</sup> <sup>b</sup>
Induced magnetization of Pd, $M_{\text{Pd}}$	$0.2 M_{\text{Co}}$ <sup>b</sup>

<sup>a</sup>Reference 8.

<sup>b</sup>Reference 9.

we obtain the domain parameters  $d$  and  $l$  within a certain precision. This simple method is quite well reproducible for a smoothly varying function.

The present theory has been applied to investigate the domain configurations of Co/Pd multilayers. Figure 2 shows the three-dimensional plot of  $\gamma_i$  as a function of the domain period  $d$  and the wall width  $l$  for  $(6\text{-}\text{\AA} \text{ Co}/11\text{-}\text{\AA} \text{ Pd})_{10}$  multilayer. The values of the magnetic parameters of Co/Pd multilayers used in the calculation are listed in Table I. The minimum  $\gamma_i$  obtained by a numerical method is indicated by the arrow, where the domain period  $d_g$  and the wall width  $l_g$  in this ground-state configuration are 200 and 8.1 nm, respectively in this particular sample. Interestingly, the ground-state domain configurations of Co/Pd multilayers were found to be very sensitive to the Co-sublayer thickness  $t_{\text{Co}}$  and a sharp transition from large domain pattern to striped one has been predicted with increasing  $t_{\text{Co}}$ .<sup>6</sup> In Fig. 3, we plot the domain period  $d_g$  and the wall width  $l_g$  in the ground-state domain configurations of  $(t_{\text{Co}}/11\text{-}\text{\AA} \text{ Pd})_{10}$  multilayers as a function of  $t_{\text{Co}}$ . In the case of  $t_{\text{Co}} \leq 2.2$  \text{\AA} (Region I), the domain period is predicted to be very large, even exceeding 1 cm. Therefore, the ground-state domain pattern in this multilayer is possibly composed of a single domain, or at least, a few large domains in the whole area of a sample. Contrastingly, a micron-scaled domain period is obtained for the condition of  $t_{\text{Co}} \geq 2.2$  \text{\AA} (Region II), where typical striped patterns are expected. In this region, the domain period is getting decreased and the wall-transition width is getting increased with increasing the Co-sublayer thickness and eventually, the system has in-plane magnetization when  $d_g/2 = l_g$  where the domains are completely occupied by domain walls. The present theory could not be applicable to the situation that  $l_g$  is larger than  $d_g/2$  and the total thickness of a multilayer is too thick to maintain the coherent magnetization direction in the sublayers.

It is worthwhile to examine the domain configuration of the Co single layer by comparing with that of Co/Pd multi-

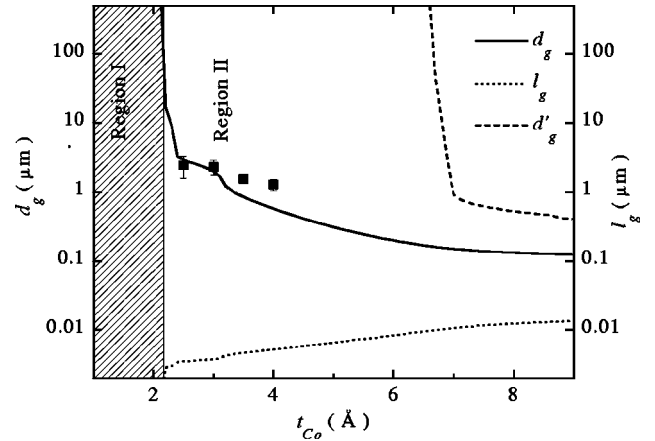


FIG. 3. The ground-state domain period  $d_g$  and the wall width  $l_g$  in  $(t_{\text{Co}}/11\text{-}\text{\AA} \text{ Pd})_{10}$  multilayers with varying  $t_{\text{Co}}$ . Regions I and II are the regions of the large-areal domain and the micron-sized stripe one, respectively. The square symbols with the error bars are the experimentally determined stripe periods and the dashed line is the ground-state domain period  $d'_g$  in the Co single-layered films.

layers. The domain configuration of the Co single layer as a limiting case of our theory was predicted by using the same values of the magnetic parameters as those of Co in Co/Pd multilayers. The dashed line  $d'_g$  in Fig. 3 represents the domain periods of Co single layered films and it shows a sharp transition with respect to the Co-layer thickness. Increasing the Co-layer thickness in the Co single layer results only in the decrement of the effective surface anisotropy density and thus, the transition of the Co single layer is essentially the same as that of the monoatomic layer calculated by the theory of Yafet and Gyorgy,<sup>6</sup> even though the two theories have been proposed by the different calculation models; the continuum model by solving Maxwell's equations and the discrete atomic model by solving the dipole interaction. In the multilayered structure, the magnetostatic energy should be reduced by interaction between the sublayers, but the magnetostatic energy in Co/Pd multilayers is largely enhanced than Co single films due to the additional polarization in nonmagnetic Pd sublayers. The magnetostatic energy distribution in the multilayered structure is very complicated but is expected to be increased with increasing the Co-sublayer thickness, while the effective anisotropy is not so much changed. Thus, the transition occurs in a similar way and it is quite understandable that the transition width of Co/Pd multilayers is much thinner than that of Co single films due to the enhancement of the magnetostatic energy from the polarization of Pd.

The transition of the magnetic domain configuration was experimentally examined by direct domain observations of a

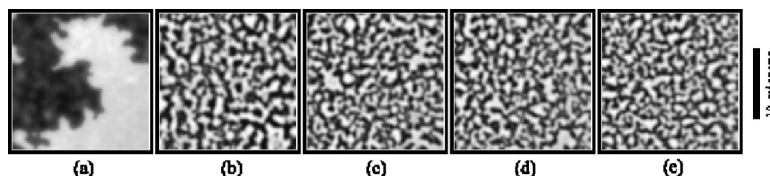


FIG. 4. The demagnetized domain configurations, captured by a magneto-optical microscope at 50% up- and 50% down-domain mixed patterns at the coercive point of the major  $M$ - $H$  hysteresis loops of  $(t_{\text{Co}}/11\text{-}\text{\AA} \text{ Pd})_{10}$  multilayers with  $t_{\text{Co}} =$  (a) 2.0, (b) 2.5, (c) 3.0, (d) 3.5, and (e) 4.0, respectively.

series of  $(t_{\text{Co}}/11\text{-\AA Pd})_{10}$  multilayers with changing  $t_{\text{Co}}$  from 2.0 to 4.0 Å with a 0.5-Å increment. The samples were prepared on glass substrates by  $e$ -beam evaporation with a 2% accuracy of the sublayer thickness.<sup>10</sup> The demagnetized domain patterns of 50% up- and 50% down-domain mixed state were obtained at the coercive point of major  $M$ - $H$  loop by a magneto-optical microscope equipped with an advanced video processing technique. In Fig. 4, we show the typical demagnetized patterns of domains in the serial samples. In the  $(2\text{-\AA Co}/11\text{-\AA Pd})_{10}$  sample, a large areal domain pattern is clearly observed as shown in Fig. 4(a). In contrast, in the samples with  $t_{\text{Co}}=2.5, 3.0, 3.5,$  and  $4.0$  Å, typical striped patterns are seen in Figs. 4(b)–4(e). The raggedness in the experimentally observed domain patterns is believed to be caused by local structural irregularities, because the domain pattern ordering force  $-(\partial\gamma_t/\partial d)$  for  $d \approx d_g$  is quite small. The measured domain periods, indicated by the square symbols with the error bars in Fig. 3, are fairly well agreed with the theoretical ones.

We believe that a sharp transition of the domain configuration in the multilayered structure is mainly ascribed to a feature of the magnetostatic energy. The ground-state domain period  $d_g$  is determined by the counterbalance between the force of  $-(\partial\gamma_d/\partial d)$  driving the domain period narrow and the force of  $-(\partial\gamma_a/\partial d + \partial\gamma_x/\partial d)$  driving the domain period wide. For the ultrathin multilayered system, the magnetostatic energy density is saturated to a value of the effective demagnetizing energy density  $2\pi M_{\text{eff}}^2$  and thus, the force of  $-(\partial\gamma_d/\partial d)$  vanishes when the domain period is over a few microns. In Fig. 5(a), we plot the total domain energy densities of  $(t_{\text{Co}}/11\text{-\AA Pd})_{10}$  with  $t_{\text{Co}}=2.0, 4.0,$  and  $6.0$  Å. The ground-state domain period  $d_g$  is increased with decreasing the magnetic-sublayer thickness, since the anisotropy energy and the exchange energy are increased while the magnetostatic energy is decreased.<sup>2</sup> When the ground-state domain period is increased up to a few microns, the domain-narrowing force of  $-(\partial\gamma_d/\partial d)$  vanishes and therefore, an enormously large domain period is realized.

It has been known that the wall configuration is mainly determined by the counterbalance of the anisotropy energy and the exchange energy. However, it should be stressed that the magnetostatic energy also plays an important role in determining the wall configuration of the multilayered structure. Figure 5(b) shows the dependences of  $\gamma_a$ ,  $\gamma_x$ ,  $\gamma_d$ , and  $\gamma_t$  on  $l$  at  $d=d_g$ . It can be noticed that the wall width  $l'_g$ , determined from only considering the anisotropy energy and the exchange energy, is much different from  $l_g$  obtained by

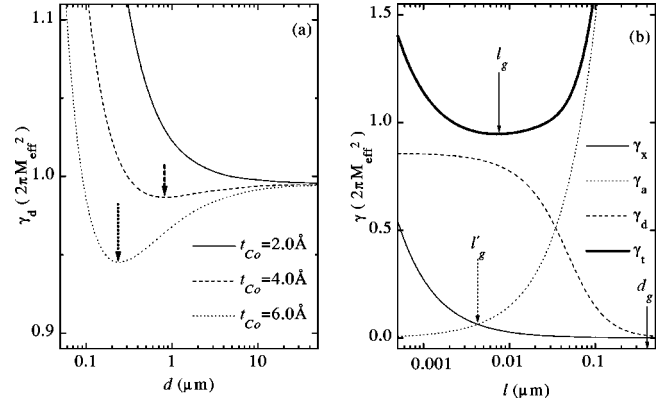


FIG. 5. (a) The plot of the total domain energy densities of  $(t_{\text{Co}}/11\text{-\AA Pd})_{10}$  multilayers with  $t_{\text{Co}}=2.0, 4.0,$  and  $6.0$  Å as a function of the domain period  $d$  at  $l=l_g$ . The ground-state domain periods  $d_g$  for each multilayer are indicated by the arrows. (b) The plot of the energy densities of  $(6\text{-\AA Co}/11\text{-\AA Pd})_{10}$  multilayers as a function of the wall width  $l$  at  $d=d_g$ . The ground-state wall width  $l_g$  is indicated by the solid arrow, while  $l'_g$  determined by considering only  $\gamma_a$  and  $\gamma_x$  is indicated by the dotted arrow.

including the magnetostatic energy. The magnetostatic energy should be taken into account unless the wall width  $l$  is much smaller than the ground-state domain period  $d_g$ , because the magnetostatic energy is not negligible for  $l \lesssim d_g$ . In this situation, the functional form of the wall-transition configuration might be different from the Bloch-wall type, which is resulted from the conventional calculation of  $l'_g$ .

In summary, we have developed a theory for the domain configurations of the magnetic multilayers by solving Maxwell's equations based on the continuum approximation. Interestingly, the domain configuration in Co/Pd multilayers was found to be very sensitively dependent on the Co-sublayer thickness and the present theory has predicted a sharp transition of the domain configuration between the large-areal domain and the striped domain configuration with varying the Co-sublayer thickness. The transition was confirmed experimentally by direct domain observation: the large-areal domains were observed in the Co/Pd multilayers of the 2-Å-thick Co sublayers, while the striped domains were observed in those of 2.5–4-Å-thick ones. We conclude that the transition occurs by saturation of the magnetostatic energy in the ultrathin magnetic sublayers.

This work was supported by Creative Research Initiatives of the Korean Ministry of Science and Technology.

<sup>1</sup>P. F. Carcia, A. D. Meinhaldt, and A. Suna, Appl. Phys. Lett. **47**, 178 (1985).

<sup>2</sup>S.-C. Shin and A. C. Palumbo, J. Appl. Phys. **67**, 317 (1990).

<sup>3</sup>M. N. Baibich, J. M. Broto, A. Fert, F. Nguyen Van Dau, F. Petroff, P. Etienne, G. Creuzert, A. Friedrich, and J. Chazelas, Phys. Rev. Lett. **61**, 2472 (1988).

<sup>4</sup>S. Honda, Y. Ikegawa, and T. Kusuda, J. Magn. Magn. Mater. **111**, 273 (1992).

<sup>5</sup>H. J. G. Draaisma and W. J. M. de Jonge, J. Appl. Phys. **62**, 3318 (1987).

<sup>6</sup>Y. Yafet and E. M. Gyorgy, Phys. Rev. B **38**, 9145 (1988).

<sup>7</sup>V. Kamberský, P. de Haan, J. Šimšová, S. Porthun, R. Gemperle, and J. C. Lodder, J. Magn. Magn. Mater. **157**, 301 (1996).

<sup>8</sup>H. P. J. Wijn, in *Data in Science and Technology*, edited by R. Poerschke (Springer-Verlag, Berlin, 1991), Chap. 1.

<sup>9</sup>J.-H. Kim and S.-C. Shin, in *Proceedings of the 3rd International Symposium on the Physics of Magnetic Materials*, edited by C. S. Kim, T. D. Lee, and J. H. Oh (The Korean Magnetic Society, Seoul, 1995), Vol. 2, p. 969.

<sup>10</sup>S.-B. Choe and S.-C. Shin, Korean Appl. Phys. **9**, 674 (1996).